Absorption and Emission Properties of Di- and Trinuclear Ruthenium(II) Rack-Type Complexes

Paola Ceroni,[a] Alberto Credi,[a] Vincenzo Balzani,*[a] Sebastiano Campagna,*[b] Garry S. Hanan,[c] Claudia R. Arana,[c] and Jean-Marie Lehn*[c]

The absorption spectra and the luminescence properties of three dinuclear Ru^{II} complexes and one trinuclear Ru^{II} complex have been investigated. All the complexes have rack-type structures. The dinuclear complexes **1**, **2**, and **3** incorporate a bis-tridentate bridging ligand made up of a pyrimidine and four pyridine moieties, as well as two 2,2′:6′,2″-terpyridyl (tpy) ligands. The trinuclear complex **4** incorporates a tris-tridentate bridging ligand made up of two pyrimidine and five pyridine moieties, as well as three tpy ligands. The absorption spectra of the complexes show a large number of ligand-centered (LC) and metal-to-ligand charge-transfer (MLCT) bands. All the complexes exhibit emission from a triplet MLCT state, with maxima in the spectral range 840–950 nm (lifetimes between 40 and 80 ns) at 298 K in fluid solution, and in the spectral range 760–810 nm (lifetimes between 2 and 3 µs) at 77 K in rigid matrices. A fine tuning of the absorption and luminescence properties of complexes **1–3** can be achieved by changing the substituents on the pyrimidine ring of the bridging ligand. Efficient energy transfer within the rack structure **4** occurs from the (upper-lying) central metal-based chromophore to the (lower-lying) peripheral ones.

Introduction

The assembly of molecular components into large, well-defined, and functional arrays (supramolecular species) is currently a major research theme.[1][2] Ruthenium(II) and osmium(II) complexes with polypyridine-type and related ligands are particularly useful units in the design of photo- and redox-active multi-component systems.[3] Some of us have recently reported the synthesis of rack-type polynuclear Ru^{II} complexes based on bis-tridentate and tris-tridentate bridging ligands made up of pyrimidine and pyridine coordinating moieties, as well as 2,2′:6′,2″-terpyridyl (tpy) ligands.[4][5] Such systems, as well as the related ladder-[6a] and grid-type[6b−6d] multi-metallic assemblies, exhibit structures of potentially great interest for the development of photonic and electronic devices.[1−3,7] We report herein the results of an investigation on the absorption spectra and luminescence properties of three dinuclear Ru^{II} complexes **1−3** and a trinuclear Ru^{II} complex **4** with rack-type structures. The synthesis and NMR characterization of the trinuclear complex are also described.

1 : R = H

2 : R = methyl

3 : R = phenyl

4
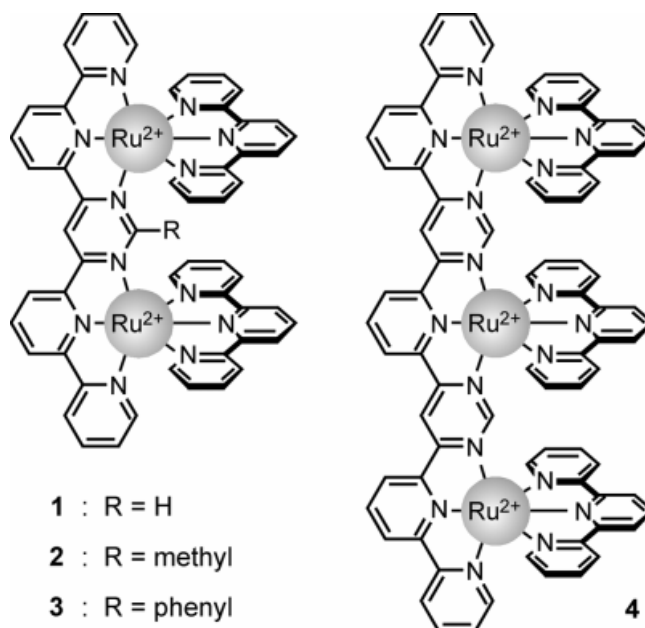
Results and Discussion

The dinucleating bis-tridentate ligands of complexes **1−3** differ only in the nature of the substituents attached at the pyrimidine unit. X-ray crystal structure analyses[4] of **1−3** have shown that the metal-to-metal distance and the center-to-center distance of the central pyridine units of the tpy ligands increase with increasing size of the substituent. Non-negligible differences have also been found in the pinching angle of the bis-tridentate ligand and in the convergence angle of the two ancillary tpy ligands. The sub-

[a] Dipartimento di Chimica "G. Ciamician",
Università di Bologna,
via Selmi 2, I-40126 Bologna, Italy
Fax: (internat.) +39-051/2099456
[b] Dipartimento di Chimica Inorganica,
Chimica Analitica e Chimica Fisica, Università di Messina,
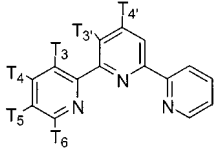Villaggio S. Agata, I-96166 Messina, Italy
Fax: (internat.) +39-090/393756
[c] Laboratoire de Chimie Supramoléculaire, Institut Le Bel,
Université Louis Pasteur,
4 rue Blaise Pascal, F-67000 Strasbourg, France

stituents can, of course, also be expected to influence the electronic properties of the ligands.

NMR Characterization of Complex 4

The proton chemical shifts measured for the three terpyridine (tpy) ligands and the tris-tridentate ligand present in **4** are collected in Tables 1 and 2, respectively. Also included in Table 1 are the chemical shift differences (in ppm) between the tpy units of complex **4** and $[Ru(tpy)_2]^{2+}$ **5** ($\Delta\delta$ **5**),[8] and in Table 2, the chemical shift differences (in ppm) between **4** and **1** ($\Delta\delta$ **1**). The importance of comparing the ^1H chemical shifts to those of a related complex rather than to those of the free ligand should be clear. Shielding effects exist between the terminal pyridines in the free ligand because of nitrogen lone pair induced helication.[9] On forming the trimetallic complex, these shielding effects are no longer present, making most of the protons in the free ligand strongly deshielded in the metal complex. The assignments were made by the following methods: comparing proton coupling constants, decoupling experiments, comparing spectra, and verifying heterocycle connectivity using NOE.[10]
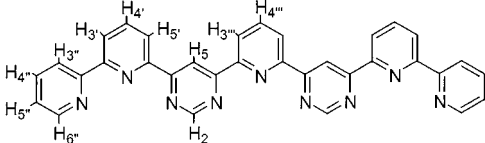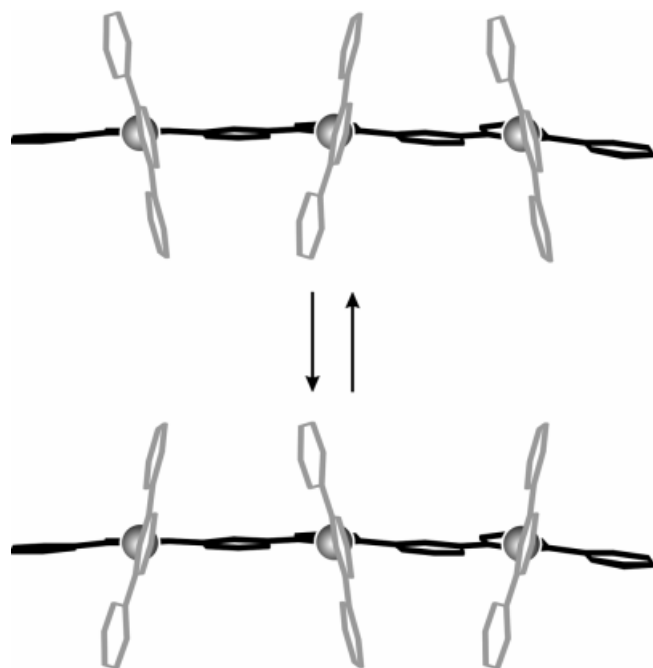
In the trimetallic complex **4**, the tpy protons are in a peripheral-to-central ratio of 2:1. The central tpy protons (H_{T*}) are more shielded than the peripheral tpy protons (H_T), as would be expected as the central tpy site is flanked by two peripheral tpy′s, whereas the peripheral tpy′s have only the central one in their vicinity.

Comparison of the chemical shifts of central pyridine in the ligand with those of the central pyridines in $[Ru(tpy)_2]^{2+}$ (**5**) allows determination of the $\Delta\delta$ **5** values for $H_{3'''}$ and $H_{4'''}$. The values are indicative of greater deshielding for $H_{3'''}$ than for $H_{4'''}$. This may be due to the preferred orientation of the terminal pyridine on the central terpyridine towards one side of the central pyridine of **L**, resulting in greater deshielding at $H_{3'''}$ and H_5 (Figure 1). The large deshielding value for H_5 in **4** as compared to **1** ($\Delta\delta$ **1**) may be explained in terms of the distorted positioning of the terminal pyridine of the central and peripheral terpyridines in **4** (Figure 1). The individual terpyridines sites in **1** are disymmetric in the solid state, as shown by the X-ray structure.[4] The terpyridines in **4** may behave similarly. This is also supported by NOE interactions, which are found between H_{T5} and H_{T5*} as well as H_{T6} and H_{T5*}. The motion represented in Figure 1, which is expected to be fast on the NMR timescale, leads to an averaged symmetry.

Absorption Spectra

The absorption spectra of compounds **1**, **2**, and **4** (acetonitrile solution, 298 K) are shown in Figures 2 and 3. The wavelengths of the absorption maxima and the values of the molar absorption coefficients for complexes **1**−**4** and the model compound $[Ru(tpy)_2]^{2+}$ (**5**) in the visible region are listed in Table 3.

The UV region of the absorption spectrum of each of the complexes is dominated by a variety of intense bands that can be assigned to ligand-centered (LC) transitions of the tpy ligands and of the multi-tridentate bridging ligands. In the visible region, several weaker bands are present, attributable to metal−to−ligand charge-transfer (MLCT) transitions.[3] At first glance, one could distinguish three types

Table 1. Proton chemical shifts (in ppm) of terpyridine ligands in **4** and chemical shift differences between **4** and $[Ru(tpy)_2]^{2+}$ **5**[a] in CD_3CN; T denotes peripheral tpy hydrogens and T* denotes central tpy hydrogens

	T6	T5	T4	T3	T3′	T4′
4 (H_T)	7.01	6.94	7.80	8.34	8.65 [b]	8.51 [b]
$\Delta\delta$ **5**	−0.32	−0.21	−0.11	−0.14	−0.09	+0.11
4 (H_{T*})	6.80 [b]	6.80 [b]	7.74	8.29	8.65 [b]	8.64 [b]
$\Delta\delta$ **5**	−0.53	−0.50	−0.17	−0.19	−0.09	+0.24

[a] Data for **5** taken from ref.[8] − [b] Central position of multiplet.

Table 2. Proton chemical shifts and chemical shift differences in the free tris-tridentate ligand **L** and **4**; for the assignments, see the sketch below

	6″	5″	4″	3″	5′	4′	3′	5	2	3‴	4‴
L [a]	8.31	6.85	6.72	8.31	8.62	8.02	8.38	9.99	9.44	8.70	8.14
4 [b]	7.27	7.14	7.92	8.46	9.12	8.51	8.82	9.92	6.15	9.20	8.64
$\Delta\delta$ **1** [c]	0	0	−0.01	+0.01	+0.01	+0.01	0	+0.66	−0.09	+0.46	+0.24
$\Delta\delta$ **5** [d]											

[a] In $CDCl_3$; data from G. S. Hanan, U. S. Schubert, D. Volkmer, E. Rivière, J.-M. Lehn, N. Kyritsakas, J. Fischer, *Can. J. Chem.* **1997**, 75, 169. − [b] In CD_3CN. − [c] Data for **1** taken from ref.[4] − [d] Data for **5** taken from ref.[8]

Figure 1. Proposed averaging motion of terpyridines in **4**

of ligand units (tpy, bpy, and pyrimidine) in the metal coordination spheres, but it should be noted that the latter two units are conjugated so that it is probably more correct to treat the multi-tridentate bridging ligands as single large molecules.[2]

Complexes 1−3: Electrochemical measurements[4] show that these complexes undergo two (metal-centered) oxidation processes at about +1.4 and +1.5 V vs. SCE, and several (ligand-centered) reduction processes. The separation between the two oxidation waves of the formally equivalent Ru[II] ions shows that the metal−metal interaction through the bis-tridentate ligands is not negligible, as is typical for this kind of bridging ligand.[3d] The first two reduction processes, which occur around −0.5 and −1.1 V,

can be assigned to successive reductions of the bridging ligand. As expected,[3a] reduction of the tpy ligands occurs at more negative potentials (around −1.5 V).
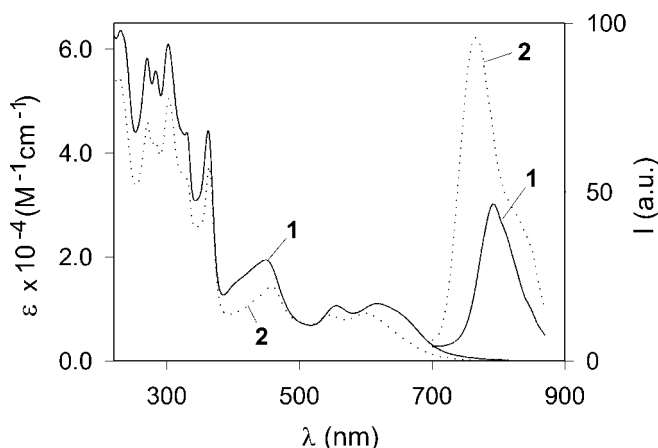
Figure 2. Absorption spectra in acetonitrile solution at 298 K (left scale) and emission spectra in a rigid butyronitrile matrix at 77 K (λ_{ex} = 480 nm; right scale) of compounds **1** and **2**

The three MLCT absorption bands observed for compounds **1−3** in the visible region (Figure 2 and Table 3) can be straightforwardly assigned in the light of the electrochemical results. The two low energy bands, with maxima around 600 and 550 nm, are due to CT transitions to the first and second LUMO′s of the bridging ligand, respectively, while the higher energy band, with a maximum at around 450 nm, is due to a transition to the first LUMO of the tpy ligands. The difference between the potentials of the first and second reduction waves is much larger than the energy separation between the two lowest energy absorption bands because the second wave is associated with reduction of an already reduced ligand. This interpretation is consistent with the results obtained for a closely related dinuclear Ru[II] rack containing an anthryl subunit.[11]

As can be seen from Figure 2, the presence of the methyl substituent on the pyrimidine ring in **2** displaces the

Table 3. Absorption and luminescence data for complexes **1−4** and for the model compound [Ru(tpy)$_2$]$^{2+}$ **5**

Compound	Absorption 298 K[a,b]		Luminescence			
			298 K[a]		77 K[c]	
	λ_{max}, nm	ε_{max}, M^{-1} cm^{-1}	λ_{max},[d] nm	τ, ns	λ_{max},[d] nm	τ, µs
1	448	19400	845	77	792	2.4
	555	10600				
	615	11000				
2	458	14700	845	51	767	3.3
	544	9900				
	597	9300				
3	457	11700	845	37	786	2.5
	555	7700				
	606	7900				
4	405[e]	25500	920	40	810[f]	2.8
	450[e]	25000				
	543	14500				
	624	19000				
[Ru(tpy)$_2$]$^{2+}$ **5**[g]	474	10400	629	< 1	598	10.6

[a] Air-equilibrated acetonitrile solution. − [b] Only the absorption bands in the visible region are indicated. − [c] Butyronitrile rigid matrix. − [d] Corrected values. − [e] Overlapping bands, see Figure 3. − [f] λ_{max} and highest energy feature of a structured band, see Figure 3. − [g] Data taken from ref.[8]

Ru→bridging ligand bands to higher energy and the Ru→tpy band to lower energy compared to the situation in **1**. This is due to the electron-donating nature of the methyl group, which has two effects: (i) it increases the electron density on the bridging ligand and therefore raises the energy of its LUMO's; (ii) by increasing the σ-donor power of the pyrimidine nitrogens, it increases the electron density on the metal and therefore decreases the energy of the MLCT band involving the tpy ligands, which are unaffected by the pyrimidine substituent. The phenyl substituent present in **3** has a similar, albeit smaller, effect.

Complex 4: In the trinuclear compound **4**, the two lateral subunits are equivalent, but different from the central one. As expected, because of the larger number of subunits, the molar absorbance is enhanced compared to that of the dinuclear compounds over the entire UV/vis domain (Figures 2 and 3, Table 3). The lowest-lying MLCT band is displaced to lower energy compared to that of the dinuclear species, due to the more extended electronic delocalization on the bridging ligand (BL), which leads to a stabilization of its LUMO. Such a low-lying MLCT band (as well as the MLCT band involving the second LUMO of the bridging ligand) should receive contributions from two different Ru→BL transitions because, as mentioned above, the peripheral Ru^{II} metal ions are different from an electronic viewpoint compared to the central Ru^{II} metal ion, since the latter is coordinated by two pyrimidine rings. The central metal ion should be more difficult to oxidize than the peripheral ones, because pyrimidines are better electron acceptors than pyridines.[12] Indeed, this was confirmed by electrochemical studies. In fact, **4** exhibits a two-electron oxidation at $+1.47$ V vs. SCE in acetonitrile solution, associated with the peripheral non-interacting metal centers, followed by a one-electron oxidation process at $+1.88$ V, attributable to oxidation of the central metal subunit.[5] Although the lowest-lying MLCT band for **4** is large and exhibits a pronounced shoulder in its red tail, the expected two bands are not resolved, probably owing to their broadness and slight energy difference (Figure 3). Interestingly, two bands are evident in the absorption spectrum of the complex in the region corresponding to the Ru→tpy CT transitions (compare the $400-500$ nm region in the absorption spectra shown in Figures 2 and 3). On the basis of the above considerations and the redox properties of **4**, these absorption bands can be assigned, in order of increasing energy, to Ru(peripheral)→tpy CT transition(s) and Ru(central)→tpy CT transition(s), respectively.

Luminescence Properties

The emission spectra of compounds **1**, **2**, and **4** (rigid butyronitrile matrix at 77 K) are shown in Figures 2 and 3. The wavelengths of the emission maxima and the excited-state lifetimes of all the complexes are collected in Table 3.

On the basis of the emission energies, spectra, and lifetimes,[3] the relatively weak emission exhibited by all the complexes can be assigned to the lowest ^{3}MLCT level,
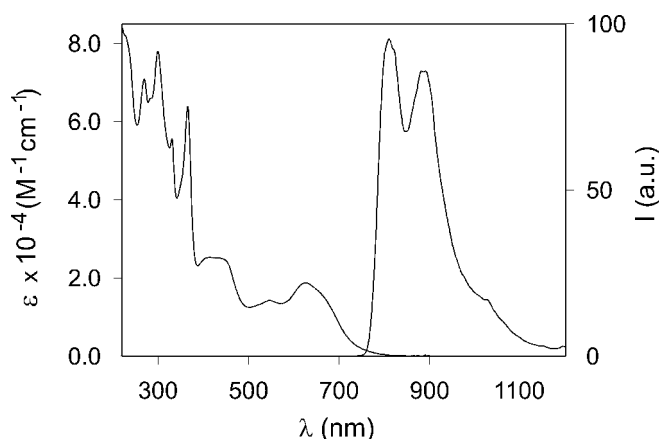

Figure 3. Absorption spectrum in acetonitrile solution at 298 K (left scale) and emission spectrum in a rigid butyronitrile matrix at 77 K (λ_{ex} = 488 nm; right scale) of compound **4**

which is associated with the bridging ligand. As already discussed for the absorption spectra, the nature of the substituent on the pyrimidine ring of the bridging ligand is responsible for fine-tuning the emission energy in **1−3**, with **2** exhibiting the highest energy emission (Table 3). The emission energy of **4** is lower than those of **1−3**, as expected considering the electronic and redox properties of the bridging ligand in **4**,[5] and according to the interpretation of the absorption data.

Compared with $[Ru(tpy)_2]^{2+}$,[3] the luminescence lifetimes of compounds **1−3** are longer at room temperature and shorter at 77 K (Table 3). This can be explained by recalling that the radiationless decay of the luminescent excited state in Ru^{II} polypyridine compounds occurs via an upper-lying metal-centered triplet (^{3}MC) level at high temperature and by vibronic coupling directly to the ground state at low temperature.[3] Since in compounds **1−3** the luminescent level is lower in energy than in $[Ru(tpy)_2]^{2+}$,[3] the activation energy for radiationless decay via the upper-lying MC level should be larger (with the reasonable assumption that in these complexes the ^{3}MC excited state has approximately the same energy), and the coupling with the ground state should be stronger. The shorter lifetime at room temperature and the longer lifetime at 77 K for **2** compared with **1** (Table 3) is in line with such an interpretation.

As mentioned above, the two metal-based chromophores of **1−3** are identical, whereas in **4** the central metal-based chromophore is different from the peripheral ones. Considering the different acceptor abilities of pyridine and pyrimidine rings and the oxidation behaviour of the complex (see above), the lowest ^{3}MLCT state of each peripheral subunit should be lower in energy than the corresponding level involving the central subunit. Because **4** contains two *different* metal-based chromophores, potentially luminescent from their respective lowest-lying ^{3}MLCT level,[3] two emissions could in principle occur. The insensitivity of the emission spectrum of **4** to the excitation wavelength (both at 77 K and at room temperature), the matching between the absorption and excitation spectra, and the pres-

ence of a single exponential luminescence decay with the same lifetime under all the experimental conditions, indicate that only the lowest-lying MLCT level of the assembly, associated with the peripheral chromophores, undergoes deactivation through radiative decay, whereas the upper-lying MLCT level, associated with the central subunit, transfers its electronic energy to the nearby chromophore. Thus, efficient energy transfer from the central chromophore to the peripheral ones occurs within the trinuclear rack.

Finally, the luminescence lifetimes of **1**−**3** at 77 K roughly obey the energy gap law,[13] but **4** exhibits a longer lifetime than expected in comparison with the dinuclear systems (**1**−**3**). This is probably due to the greater delocalization of the acceptor ligand of the MLCT luminescent level in **4**, which decreases the vibronic coupling between excited and ground states, thereby reducing the Franck−Condon factors for non-radiative decay.[14]

Conclusion

The absorption spectra and the luminescence properties of one trinuclear and three dinuclear ruthenium(II) rack-type complexes have been studied. The absorption spectra of the complexes show a multitude of LC and MLCT bands. All the complexes exhibit luminescence from the lowest-lying ^{3}MLCT level, both at 298 K in fluid solution and at 77 K in rigid matrices. The absorption and emission properties of the dinuclear compounds **1**−**3** are fine-tuned by the substituents on the pyrimidine ring incorporated in the bridging ligand framework. Excited-state decays are governed by direct vibronic coupling with the ground state at 77 K and by thermally-activated population of a close-lying ^{3}MC level at room temperature. In **4**, efficient electronic energy transfer occurs from the upper-lying central chromophore to the lower-lying peripheral ones. This result is of interest with regard to the possible development of larger (disymmetric) racks exhibiting vectorial energy and/or electron transfer within their structures

Experimental Section

The syntheses, characterization, and structures of compounds **1**−**3** have been described in detail elsewhere;[4] synthetic procedures for the preparation of **4** have also been outlined previously.[5] NMR instrumentation and methods used were as reported previously.[4]

Absorption and Luminescence Measurements: Absorption spectra were recorded with a Perkin−Elmer λ6 spectrophotometer in acetonitrile solution at room temperature. Luminescence experiments were performed in dilute (ca. 10^{-5} M) acetonitrile solution at room temperature and in rigid butyronitrile matrices at 77 K. Corrected luminescence spectra in the 700−850 nm range were obtained with a Perkin−Elmer LS-50 spectrofluorimeter. Corrected luminescence spectra in the 800−1200 nm range were obtained with an in-house constructed near-infrared spectrofluorimeter consisting of an Ar ion laser as excitation source (λ_{ex} = 488 nm), a monochromator (Edinburgh) with a grating of 1200 L/mm, and a liquid nitrogen cooled germanium detector and preamplifier (Northcoast, model EO-817 L). The sample (air-equilibrated

CH$_3$CN solution) was placed in a 10 mm × 10 mm cuvette, and a beam chopper (Stanford Research, model SR540) was placed between the excitation source and the sample; luminescence was monitored at right angles to the excitation. A muon filter (Northcoast, model 829B) was used as an electronic signal filter, after the signal had been sent to a lock−in amplifier (Stanford Research, model SR510). Luminescence lifetimes were measured with an Edinburgh single-photon counting apparatus (D$_2$ lamp, λ_{ex} = 310 nm). Estimated errors are as follows: molar absorption coefficients, 10%; absorption maxima, ±2 nm; emission maxima in the visible range, ±2 nm; emission maxima in the near-infrared range, ±4 nm; emission quantum yields, 20%; excited-state lifetimes, 10%.

Preparation of Complex 4: To Ru(tpy)Cl$_3$ (0.0324 g, 0.0735 mmol) and free tris-tridentate ligand (0.0102 g, 0.0188 mmol) was added propan-2-ol/water (20 mL, 1:1) and *N*-ethylmorpholine (0.5 mL). The mixture was heated under reflux for 40 h, then cooled to room temperature and filtered. Excess aqueous NH$_4$PF$_6$ was added to the solution and the precipitate was collected. The solid was purified by successive recrystallizations from acetonitrile/toluene to afford **4** (0.0264 g, 58%) as a green solid. − M.p. > 300°C. − ^{1}H NMR (CD$_3$CN, 400 MHz); the subscript T indicates protons of the peripheral terpyridine ligands and T* indicates protons of the central terpyridine ligand: δ = 9.29 (s, 1 H, H$_5$), 9.20 (d, *J* = 8.4 Hz, 2 H, H$_{3''}$), 9.12 (d, *J* = 8.4 Hz, 2 H, H$_{5'}$), 8.82 (d, *J* = 8.2 Hz, 2 H, H$_{3'}$), 8.65 (d, *J* = 8.4 Hz, 6 H, H$_{T3', T3'*}$), 8.64 (m, 2 H, H$_{4''',T4'*}$), 8.51 (m, 4 H, H$_{4',T4'}$), 8.46 (d, *J* = 7.2 Hz, 2 H, H$_{3''}$), 8.34 (d, *J* = 8.2 Hz, 4 H, H$_{T3}$), 8.29 (d, *J* = 8.0 Hz, 2 H, H$_{T3*}$), 7.92 (td, *J* = 7.8, 1.5 Hz, 2 H, H$_{4''}$), 7.80 (td, *J* = 8.0, 1.5 Hz, 4 H, H$_{T4}$), 7.74 (td, *J* = 8.2, 1.9 Hz, 2 H, H$_{T4*}$), 7.27 (d, *J* = 5.0 Hz, 2 H, H$_{6''}$), 7.14 (ddd, *J* = 7.5, 5.7, 1.2 Hz, 2 H, H$_{5''}$), 7.01 (d, *J* = 5.5 Hz, 4 H, H$_{T6}$), 6.94 (ddd, *J* = 7.4, 5.7, 1.5 Hz, 4 H, H$_{T5}$), 6.80 (m, 4 H, H$_{T6*,T5*}$), 6.15 (d, *J* = 0.8 Hz, 1 H, H$_2$). − ^{13}C{^{1}H} NMR (CD$_3$COCD$_3$, 100 MHz): δ = 166.89, 165.32, 161.39, 158.43, 157.96, 157.07, 156.89, 155.57, 155.07, 154.67, 154.51, 153.92, 153.81, 153.16, 140.31, 140.16, 139.68, 139.65, 138.64, 137.13, 136.97, 129.59, 128.95, 128.86, 128.67, 127.93, 126.83, 125.67, 125.19, 124.98, 124.50, 118.50 (one overlapped resonance). − FAB: *m/z* (%): 2272 (40) [M − PF$_6$]$^+$, 2126 (100) [M − 2 PF$_6$]$^+$, 1981 (62) [M − 3 PF$_6$]$^+$, 1063 (36) [M − 2 PF$_6$]$^{2+}$, 991 (78) [M − 3 PF$_6$]$^{2+}$, 918 (33) [M − 4 PF$_6$]$^{2+}$. − C$_{78}$H$_{54}$F$_{36}$N$_{18}$P$_6$Ru$_3$·4CH$_3$CN: calcd. C 40.02, H 2.58, N 11.94; found C 40.33, H 2.81, N 11.40.

Acknowledgments

[1] J.-M. Lehn, *Supramolecular Chemistry: Concepts and Perspectives*, VCH, Weinheim, **1995**.
[2] V. Balzani, F. Scandola, *Supramolecular Photochemistry*, Ellis Horwood, Chichester, **1991**.
[3] [3a] A. Juris, V. Balzani, F. Barigelletti, S. Campagna, P. Belser, A. Von Zelewsky, *Coord. Chem. Rev.* **1988**, *84*, 85. − [3b] T. J. Meyer, *Acc. Chem. Res.* **1989**, *22*, 163. − [3c] J.-P. Sauvage, J.-P. Collin, J.-C. Chambron, S. Guillerez, C. Coudret, V. Balzani, F. Barigelletti, L. De Cola, L. Flamigni, *Chem. Rev.* **1994**, *94*, 993. − [3d] V. Balzani, A. Juris, S. Campagna, S. Serroni, *Chem. Rev.* **1996**, *96*, 759.
[4] G. S. Hanan, C. R. Arana, J.-M. Lehn, G. Baum, D. Fenske, *Chem. Eur. J.* **1996**, *2*, 2019.

[5] G. S. Hanan, C. R. Arana, J.-M. Lehn, D. Fenske, *Angew. Chem. Int. Ed. Engl.* **1995**, *34*, 1122.

[6] [6a] P. N. W. Baxter, G. S. Hanan, J.-M. Lehn, *J. Chem. Soc., Chem. Commun.* **1996**, 2019. − [6b] P. N. W. Baxter, J.-M. Lehn, J. Fischer, M.-T. Youinou, *Angew. Chem. Int. Ed. Engl.* **1994**, *33*, 2284. − [6c] G. S. Hanan, D. Volkmer, U. S. Schubert, J.-M. Lehn, G. Baum, D. Fenske, *Angew. Chem. Int. Ed. Engl.* **1997**, *36*, 1842. − [6d] A. Garcia, F. Romero-Salguero, D. M. Bassani, J.-M. Lehn, G. Baum, D. Fenske, *Chem. Eur. J.* **1999**, *5*, 1803.

[7] See also, for example: [7a] O. Waldmann, J. Hassmann, P. Müller, G. S. Hanan, D. Volkmer, U. S. Schubert, J.-M. Lehn, *Phys. Rev. Lett.* **1997**, *78*, 3390. − [7b] D. Astruc, *Acc. Chem. Res.* **1997**, *30*, 383.

[8] M. Maestri, N. Armaroli, V. Balzani, E. C. Constable, A. M. W. Cargill Thompson, *Inorg. Chem.* **1995**, *34*, 2759.

[9] G. S. Hanan, J.-M. Lehn, N. Kyritsakas, J. Fischer, *J. Chem. Soc., Chem. Commun.* **1995**, 765.

[10] Trimetallic complex **4** exhibits all of the expected interannular NOE interactions.

[11] A. Credi, V. Balzani, S. Campagna, G. S. Hanan, C. R. Arana, J.-M. Lehn, *Chem. Phys. Lett.* **1995**, *243*, 105.

[12] P. Ford, D. F. D. Rudd, R. Gaunder, H. Taube, *J. Am. Chem. Soc.* **1968**, *90*, 1187.

[13] [13a] W. Siebrand, *J. Chem. Phys.* **1967**, *46*, 440. − [13b] J. V. Caspar, E. M. Kober, B. P. Sullivan, T. J. Meyer, *J. Am. Chem. Soc.* **1982**, *104,* 630. − [13c] J. V. Caspar, T. J. Meyer, *J. Phys. Chem.* **1983**, *87*, 952. − [13d] T. J. Meyer, *Pure Appl. Chem.* **1986**, *58*, 1193.

[14] [14a] G. F. Strouse, J. R. Schoonover, R. Duesing, S. Boyde, W. E. Jones Jr., T. J. Meyer, *Inorg. Chem.* **1995**, *34*, 473. − [14b] A. C. Benniston, V. Grosshenny, A. Harriman, R. Ziessel, *Angew. Chem. Int. Ed. Engl.* **1994**, *33*, 1884.